

Experimental validation of the Helmholtz equation for the surface potential of Langmuir monolayers

Abdel I. El Abed*

Laboratoire de Neuro-Physique Cellulaire (LNPC), Université Paris Descartes, 45 rue des Saints-Pères, 75006 Paris, France

(Received 12 June 2009; published 6 October 2009)

We show in this paper that monolayers of the nonhydrophilic F_8H_{18} semifluorinated n -alkane constitute when spread on the hydrophobic top of an alamethicin Langmuir monolayer, a very good experimental system in order to check the validity of Helmholtz equation. This system allows for a good agreement between measured and calculated surface potentials of unionized Langmuir monolayers. We show also that the relative dielectric constant of the F_8H_{18} monolayer does not vary upon compression of the monolayer, the measured 2.9 value is in a very good agreement with literature data. We attribute this behavior to the self-aggregation of F_8H_{18} molecules in nanosized circular domains whose size remains constant upon compression as shown by atomic force microscopy.

DOI: [10.1103/PhysRevE.80.041601](https://doi.org/10.1103/PhysRevE.80.041601)

PACS number(s): 68.18.Fg, 68.55.-a, 61.30.Hn

I. INTRODUCTION

The surface potential (ΔV) of unionized Langmuir monolayers (LMs) [1] may be expressed easily versus molecular area A , according to the modified Helmholtz formula [1,2]:

$$\Delta V = \frac{\mu_z}{A\epsilon_0\epsilon}, \quad (1)$$

where μ_z , ϵ_0 , and ϵ represent the average vertical component of the molecular dipole moment $\vec{\mu}$, the permittivity of free space, and the relative dielectric constant of the monolayer, respectively. ϵ may be considered as an *apparent* relative permittivity which accounts for dipole-dipole interactions within the monolayer [3].

Whereas measurements of ΔV - A isotherm diagrams of LMs are relatively easy to implement, their accurate interpretation remains generally very difficult to achieve. Indeed, due to the large difference which exists between the relative dielectric constant of water and air, it is very difficult to estimate ϵ values of Langmuir monolayers. Thus, one can deduce, generally, only an *effective* value of the vertical component of the molecular electric dipole moment, μ_z/ϵ . Moreover, the water surface above which the monolayer spreads is itself polarized by spontaneous orientation of water molecules. Thus, while compressing the amphiphilic monolayer at the air-water interface, the recorded ΔV could result either from reorientation of hydrophobic chains, or/and a change in conformation of hydrophilic head groups, or/and the reorientation of water molecules underneath the monolayer. This is particularly true in the case of the classical amphiphilic Langmuir monolayers where the hydrophilic head group undergoes a strong interaction with the water subphase. However, a considerable progress has been made on the understanding of surface potential measurements on both experimental and theoretical levels. For instance, Taylor *et al.* showed that reproducible ΔV - A isotherm diagrams could be obtained if the water employed in the subphase is ad-

equately purified [4]. Demchak and Fort (DF) [3] suggested an electric model, in which the monolayer may be considered as a three layer capacitor with distinct dielectric constants:

$$\Delta V = \frac{1}{A\epsilon_0} \left(\frac{\mu_1}{\epsilon_1} + \frac{\mu_2}{\epsilon_2} + \frac{\mu_3}{\epsilon_3} \right), \quad (2)$$

where μ_1 is the normal component of the dipole moment due to the reorientation of the water molecules owing to the presence of the monolayer, μ_2 is the normal component of the dipole moment from the hydrophilic head groups at the monolayer-water interface, and μ_3 is the normal component of the dipole moment from the hydrophobic tail groups at the monolayer/air interface [5]. ϵ_i are the effective dielectric constants of the respective regions in which the dipoles are located. Demchak and Fort [3] suggested $\epsilon_2=7.6$ and $\epsilon_3=5.3$. Later, Oliveira *et al.* [6] showed that for monolayers composed of long aliphatic chains $\epsilon_2=6.4$ and $\epsilon_3=2.8$ would be more appropriate values.

As argued above, due to the limitations associated with the use of the polar water subphase and classical amphiphilic molecules, another experimental system is needed for a better agreement between measured and calculated surface-potential measurements. For instance, monolayers made of semifluorinated n -alkanes (SFA), $F(CF_2)_n(CH_2)_mH$ (denoted F_nH_m) [7–10], which may spread on the nonpolar alkane liquid subphase, would be a good candidate. Indeed, an interesting feature of SFA, owing to the presence of both an oleophilic and an oleophobic chains, is their ability to exhibit surface activity at the liquid alkane-air interface [11–14]. Unfortunately, since the free energy of transfer of one $-CH_2-$ group from an alkane solvent to a perfluorinated alkane solvent (1.1 kJ mol^{-1}) is only one third of the energy needed to transfer a $-CH_2-$ group from an alkane solvent to water [12], attempts to obtain condensed SFA Langmuir monolayers at the liquid alkane-air interface have failed.

More recently, it has been shown that SFA molecules may organize also as monolayers on the hydrophobic top of phospholipid [15] and alamethicin [16,17] Langmuir monolayers. Alamethicin is a natural α -helix peptide (alam) which forms

*abdel.elabed@parisdescartes.fr

stable Langmuir monolayers at the air-water interface [18,19]. The two-dimensional crystalline structure and the suitable collapse properties of the underlying alamethicin monolayer allow for a continuous compression of the F_8H_{18} monolayer on the top of the underlying alamethicin monolayer whose density remains constant.

In this paper, we show by combining surface pressure, surface-potential measurements, and atomic force microscopy (AFM) that monolayers of perfluorooctyl *n*-octadecane, $F(CF_2)_8-(CH_2)_{18}H$ (labeled F_8H_{18}), spread on the top of alamethicin Langmuir monolayer, constitute a very good model which allow for a good agreement between measured and calculated surface-potential isotherm diagrams. We show also that the relative dielectric constant of the F_8H_{18} monolayer does not vary upon compression in this particular system. We attribute this result to the self-aggregation of F_8H_{18} molecules in nanosized circular domains whose size remains constant upon compression as observed by atomic force microscopy.

II. EXPERIMENT

The used $F(CF_2)_8-(CH_2)_{18}H$ compound was synthesized and purified (>98%) by M. Sanière from the Laboratoire de Chimie Pharmacologique et Toxicologique, Université Paris 5. Its preparation was carried out according to a well-known procedure [7]. At ambient temperature, it exhibits a crystalline phase which melts to an isotropic liquid at a temperature equal to 53 °C.

F_8H_{18} molecules possess an overall electric dipole moment μ_F intensity of about 2.8 D as calculated by Broniatowski *et al.* [20] and by Fujiwara *et al.* [21]. It is oriented from the fluorocarbon bloc toward the hydrocarbon bloc and makes a tilt angle of 35° by regards to the molecular long axis. It is mainly due to the CF_2-CH_2 junction and to the terminal $-CF_3$ group.

The rodlike α -helix alamethicin is a natural antibiotic peptide constituted by 19 amino-acid residues and one amino alcohol. In our study, it may be approximated by a cylinder of a 1.0 nm diameter and a 3.0 nm height. The biological property of alamethicin relies on its amphiphilic feature and its ability to form ionic channels across the biological cell membrane. The majority of the alamethicin amino-acid residues, including the N-terminus, are hydrophobic in nature. The peptide is amphiphilic since its polar hydrophilic groups are either at the C-terminus or lies along a narrow hydrophilic strip parallel to the helix axis. The used alamethicin compound was purchased from Sigma (Mw. 1959.9) and used as received.

The surface potential (ΔV) versus molecular area A isotherm diagrams were recorded simultaneously with $\pi-A$ isotherm diagrams using a Langmuir trough purchased from Nima Technology Ltd. The surface potential sensor consists of a Nima Kelvin probe with an area of 0.2 cm² which is suspended above the film at the air-water interface. It consists of a Kelvin vibrating-probe specifically designed to characterize Langmuir monolayers as described in detail by I. Peterson in Ref. [22]. The surface-potential sensor is based on a piezodriven tuning-fork assembly gold-plated electrode

and includes a high-gain low-noise preamplifier to maximize sensitivity and minimize parasitic coupling. A manual compensation control allows the systematic measurement offsets originating in the electronics to be nulled. Surface potential and molecular areas were measured with an accuracy of 30 mV and 5%, respectively.

The surface pressure was measured using a Wilhelmy plate with an accuracy of about 0.1 mN/m. Monolayers were obtained from a 2.5 mM chloroform F_8H_{18} solution and a 1.0 mM chloroform alamethicin solution which were mixed before spreading and then spread together on a pure water surface ($pH=5.7$). The films were compressed at a constant compression rate of 2 cm²/min. The experiments were performed at $T=20$ °C.

The mixed films were also transferred onto silicon substrates using the Langmuir-Blodgett (LB) technique, in order to be imaged with an AFM. The used AFM was a Nanoscope III, and the transferred films were analyzed in the tapping mode. The solid supported films were imaged soon after having been transferred. The used silicon wafers were mildly cleaned using a detergent sonicated bath, ethanol/water solutions, and then abundantly rinsed with purified water. In these conditions, silicon wafers are hydrophilic since the native thin oxide layer which forms onto their surface in contact with air is not removed by HF acid treatment. The transferred films were observed to be stable during AFM imaging experiments, i.e., ~ 1 h. We did not study their stability during longer periods of time.

Because alamethicin and F_8H_{18} molecules demix spontaneously, as shown previously [16,17], along the normal to the air-water interface when mixed together, we have to distinguish between F_8H_{18} molecular areas, A_F , and alamethicin molecular areas, A_{alam} , which we define as $A_F=S/n_F$ and $A_{alam}=S/n_{alam}$, where S , n_F , and n_{alam} represent the overall film area S , the number of F_8H_{18} , and alamethicin molecules, respectively. Also, we define $R_{F/alam}=n_F/n_{alam}$ as the $F_8H_{18}/alam$ molecular mixture ratio. Thus, to convert for instance the $\pi-A$ isotherm diagram x axis from A_F to A_{alam} , one should simply multiply A_F values by the considered $R_{F/alam}$ value.

III. RESULTS AND DISCUSSION

A. Characterization of the supporting alamethicin monolayer

Curve (a) of Fig. 1(A) shows the $\pi-A$ isotherm diagram of a pure alamethicin monolayer. It indicates that the alamethicin molecules form a dense monolayer at a surface pressure of about 20 mN/m and a molecular area of about 3.20 nm². In this phase, as shown in detail in previous studies [18,19], molecules organize in a 2D crystalline rectangular lattice where the alamethicin α -helix axis aligns parallel to the air/water interface. The most important feature of the alamethicin monolayer, for the present study, is that upon further compression, the $\pi-A$ isotherm diagram exhibits a collapse plateau region at about $\pi=30$ mN/m, which corresponds to a solubilization process versus compression, of the alamethicin molecules into the water subphase [18,19]. In this plateau region, the density of alamethicin molecules remains constant as corroborated by surface-potential measure-

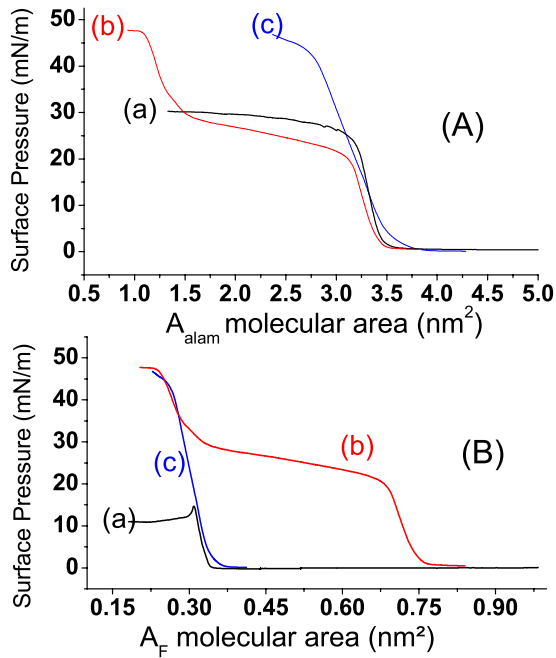


FIG. 1. (Color online) Surface pressure π versus A_{alam} (figure A) and A_F (figure B) isotherm diagrams of the pure alamethicin monolayer (curve A-a), the pure F_8H_{18} monolayer (curve B-a) and two mixed F_8H_{18} /alamethicin films with two different molecular mixture ratios: $R_{F/alam}=3.68$ (curve b) and $R_{F/alam}=11.06$ (curve c); the compression rate was about $2 \text{ cm}^2/\text{min}$ and the temperature was set at $T=20 \text{ }^\circ\text{C}$.

ments, shown in Fig. 4(A)-curve (a). The positive sign of the recorded ΔV shows that the normal component $\mu_{alam,\perp}$ of the alamethicin electric dipole moment μ_{alam} is oriented upwards. From the measured value $\Delta V=0.540 \text{ mV}$ at $A_{alam}=3.20 \text{ nm}^2$, one could deduce the effective normal component value of the alamethicin monolayer dipole moment: $\mu_{alam,\perp}/\epsilon_{alam}=4.62 \text{ D}$.

B. Structural characterization of mixed F_8H_{18} and alamethicin monolayers

Despite the missing of a hydrophilic group in SFA molecules, stable monolayers of these molecules can be obtained

at the air-water interface. We would like to present first the π - A isotherm diagram of the pure F_8H_{18} monolayer spread at the air-water interface, see curve (a) of Fig. 1(B). It shows the existence of a stable dense phase at a molecular area of about 0.30 nm^2 , which is very close to the cross section of fluorinated chains (0.28 nm^2) whose structure was studied by many authors [11,20,23–26] (see for a recent review Refs. [27,28]).

The curves (b) of Figs. 1(A) and 1(B) show the π - A isotherm diagram of a mixed alam/ F_8H_{18} film, with $R_{F/alam}=3.68$, versus A_{alam} and A_F molecular areas (as defined in the experimental section), respectively. We notice that the surface pressure π increases steeply at an alamethicin molecular area A_{alam} of about 3.2 nm^2 as like as for the pure alamethicin monolayer [Fig. 1(A)]. On compressing the film further, a second increase in surface pressure occurs around $\pi=45 \text{ mN/m}$ and $A_F \sim 0.28 \text{ nm}^2$, as like as for the pure F_8H_{18} film [Fig. 1(B)]. The first increase in surface pressure corresponds to the compression of a pure alamethicin monolayer and the second increase in surface pressure corresponds to the compression of pure F_8H_{18} monolayer. Such a behavior originates from the spontaneous vertical phase separation between F_8H_{18} and alamethicin molecules and the formation of a F_8H_{18} monolayer on the top of the alamethicin monolayer as discussed in detail in a previous study [16].

The curves (c) of Figs. 1(A) and 1(B) correspond to a particular case where $R_{F/alam} \approx 11$ for which the underlying alam monolayer should be fully covered by F_8H_{18} molecules. Indeed, the molecular mixture ratio can be expressed also as $R_{F/alam} = A_{0,alam}/A_{F_0} = 11.06$, where $A_{0,alam} = 3.20 \text{ nm}^2$ and $A_{F_0} = 0.28 \text{ nm}^2$ represent molecular areas of the close-packed pure alam and F_8H_{18} monolayers, respectively. In this case, the surface pressure increases steadily from 0 mN/m up to 45 mN/m at a molecular area of about 0.3 nm^2 .

In order to give a better view of the structure of the mixed films, we present in Fig. 2 AFM images of two different alam/ F_8H_{18} films which were transferred, onto silicon substrates using the Langmuir-Blodgett technique [1]. Figure 2(a) shows the AFM image transferred at $\pi=24 \text{ mN/m}$ ($A_F \approx 0.6 \text{ nm}^2$) while Fig. 2(b) shows the image transferred at $\pi=34 \text{ mN/m}$ ($A_F \approx 0.3 \text{ nm}^2$). Analysis of these images shows that F_8H_{18} molecules form, on the top of the underly-

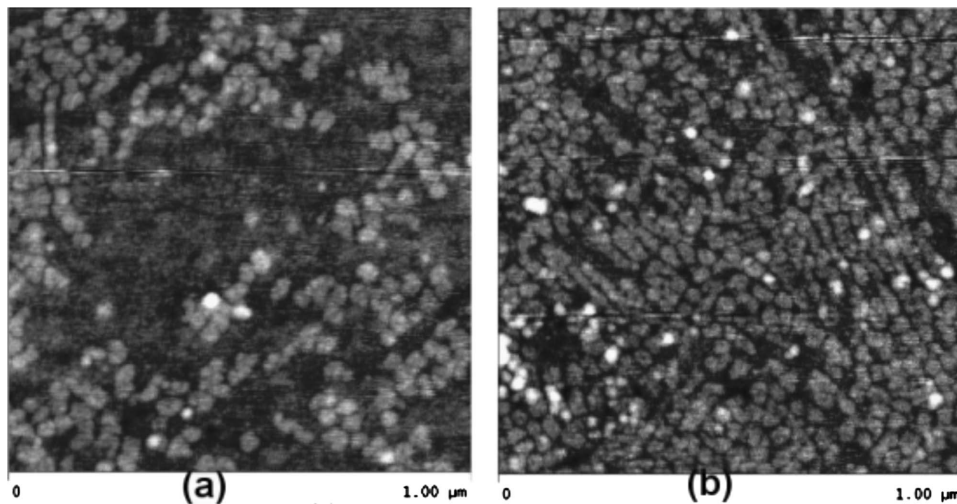


FIG. 2. AFM images of two alam/ F_8H_{18} mixed bilayers transferred at (a) $A_F=0.6 \text{ nm}^2$, the F_8H_{18} monolayer occupy roughly half of the overall surface as expected, (b) $A_F=0.3 \text{ nm}^2$, an almost densely packed monolayer of F_8H_{18} molecules can be observed.

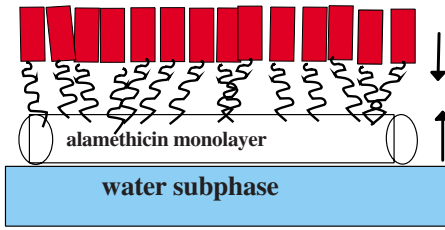


FIG. 3. (Color online) Schematic representation of the used monolayer model system which consists on the spontaneous organization of an upper F_8H_{18} monolayer on the top of alamethicin monolayer. Arrows indicate the direction of the vertical components of the molecular dipole moments.

ing alamethicin monolayer, nanosized circular domains with a characteristic diameter size of about 4.0 nm and a thickness approximately equal to 2.6 nm. As we can notice, at the smaller A_F value of 0.3 nm², a close-packed monolayer of F_8H_{18} molecules with a similar nanoscopic pattern can be observed [Fig. 2(b)]. The measured thickness value of 2.6 nm is in agreement with the monolayer organization model sketched in Fig. 3. In such organization, the F_8H_{18} molecules point their fluorinated blocs upwards and align their long molecular axis normally to the air-water interface. Such an organization has been shown previously in more detail using grazing x-ray reflectivity [16] and grazing x-ray diffraction [17]. Taking account of the calculated value of the electric dipole moment of semifluorinated n -alkanes, $\mu_F = 2.8$ D, and its orientation by regards to the long molecular axis, 35° [20], one may deduce the vertical component of the F_8H_{18} electric dipole moment: $\mu_{F,\perp} \approx 2.3$ D for these mixed films.

C. Measured and calculated surface potential isotherm diagrams of mixed F_8H_{18} and alamethicin monolayers

Curves (b–d) of Figs. 4(A) and 4(B) show the ΔV – A isotherm diagrams of the alam/ F_8H_{18} mixed films versus A_{alam} and A_F for different molecular mixture ratios: $R_{F/alam} = 3.68$, $R_{F/alam} = 7.06$, and $R_{F/alam} = 11.06$, respectively. As we can notice, the greater the density of the upper F_8H_{18} monolayer the lower the surface potential of the mixed film. Such a result indicates that the surface potential of the upper F_8H_{18} layer is negative and thus F_8H_{18} molecules should orient their electric dipole moment downward, i.e., fluorinated segments should be oriented upward and hydrocarbon segments should be oriented downward as sketched in Fig. 3.

In order to analyze these results, we consider, using the Demchak and Fort model [3], the mixed alamethicin/ F_8H_{18} film as a two-layer capacitor where the lower and the upper layers are those of alamethicin and F_8H_{18} , to which we assign respectively two relative dielectric constants ϵ_{alam} and ϵ_F and two dipole moments $\mu_{alam,\perp}$ and $\mu_{F,\perp}$. Thus, the surface potential of the alamethicin/ F_8H_{18} film may be expressed as follows:

$$\epsilon_0 \Delta V = \frac{\mu_{alam,\perp}}{\epsilon_{alam} A_{alam}} + \frac{\mu_{F,\perp}}{\epsilon_F A_F}, \quad (3)$$

where ΔV and A_F are expressed in V and nm², respectively; $\mu_{alam,\perp} / \epsilon_{alam} = 4.62$ D and $A_{alam} = 3.2$ nm² in the π – A isotherm region of interest [29].

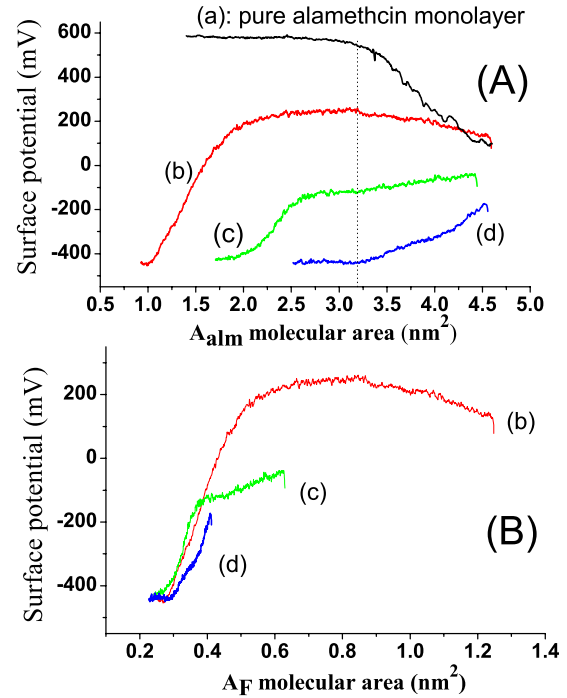


FIG. 4. (Color online) Surface potential ΔV versus A_{alam} (figure A) and A_F (figure B) isotherm diagrams of the pure alamethicin monolayer (curve A-a) and of the F_8H_{18} /alamethicin mixed films: $R_{F_8H_{18}/alam} = 3.68$ (curve b), $R_{F_8H_{18}/alam} = 7.06$ (curve c), and $R_{F_8H_{18}/alam} = 11.06$ (curve d). The vertical dot line shows the A_{alam} molecular area value, 3.20 nm², at which ΔV values used to plot ΔV versus A_F^{-1} as represented in Fig. 5.

As stated above, the estimation of ϵ_F value is more difficult. Macdonald and Barlow [4] gave a simple evaluation of the relative dielectric constant ϵ of LMs as a function of the monolayer smallest intermolecular distance a (given in Å) and, therefore, of the molecular area A :

$$\epsilon = 1 + \frac{11.0342}{a^3} \alpha, \quad (4)$$

where α represents the monolayer electronic polarizability (given in $4\pi\epsilon_0 \text{ \AA}^3$). Taylor *et al.* [3] used the image dipoles method to take into account the contribution of the subphase. Later, Iwamoto and co-workers [30] suggested to take account of both contributions of the subphase and the orientational distribution $f(\cos \theta)$ of the monolayer molecules at a given monolayer dipole moment tilt angle θ . These authors showed that the monolayer *effective* relative dielectric constant ϵ may be expressed as follows:

$$\epsilon = 1 + \frac{11.0342}{a^3} \alpha \frac{2\epsilon_s}{\epsilon_s + 1} + \frac{11.0342}{a^3} \left(\frac{2\epsilon_s}{\epsilon_s + 1} \right) \frac{1}{4\pi\epsilon_0} \frac{\mu^2 (1 - \cos \theta)^2}{12kT}, \quad (5)$$

where ϵ_s represent the relative dielectric constant of the subphase and where a and α represent respectively the smallest intermolecular distance and the monolayer electronic polar-

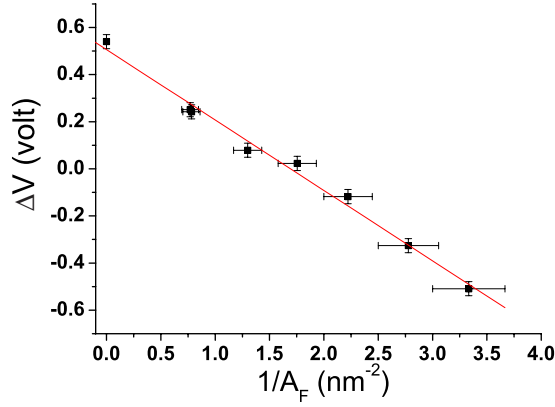


FIG. 5. (Color online) Plot of surface potential ΔV versus A_F^{-1} . The different values of ΔV were measured from different mixed F_8H_{18} /alamethicin films at a fixed alamethicin molecular area of $A_{alam}=3.20 \text{ nm}^2$, with $R_{F/alam}$ varying from 2.46 to 11.

izability. According to either Eq. (4) or Eq. (5), the value of ϵ_F should vary versus a^{-3} , i.e., $A_F^{-3/2}$.

Nevertheless, one should note that Eq. (5) has been established assuming a uniform assembly of equally separated dipoles, whereas in our case, as seen from AFM images, the monolayer consists of nanosized domains within which molecules are closely packed. Thus, the relative dielectric constant ϵ_F in our case should be more likely comparable to that of a condensed monolayer. Moreover, if one plots the measured surface potential ΔV versus A_F^{-1} (Fig. 5), one observes a linear variation ΔV versus A_F^{-1} which indicates that the relative dielectric constant ϵ_F of the F_8H_{18} monolayer does not depend on the A_F molecular area value. The determination of the slope value of the obtained linear curve ΔV versus A_F^{-1} gives the value of the effective electric dipole moment of F_8H_{18} molecules: $\mu_{F,\perp}/\epsilon_F = -0.78 \text{ D}$ which gives in turn an experimental value for the relative dielectric constant of the F_8H_{18} monolayer of about $\epsilon_F = 2.9$. It is interesting to note that such a value is very close to the 2.8 value suggested by Oliveira *et al.* for the μ_3 relative dielectric constant of a monolayer made of long aliphatic chains [6].

We calculate the film surface potential versus A_F molecular area by substituting $\frac{\mu_F}{\epsilon_F}$ in Eq. (3) with the measured constant value of -0.78 D . The corresponding diagram is shown in Fig. 6 curve (b). We calculate also the film surface potential in the case where ϵ_F is considered as a function of the intermolecular distance a , given by Eq. (5). The corresponding diagram is shown in Fig. 6 curve (c). In the former case, we calculate the ϵ_F value from Eq. (5) by assuming an hexagonal organization of the molecules in the monolayer and by replacing $\mu_{F,\perp}$ by the above calculated 2.3 D value. The electronic polarizability α of the F_8H_{18} monolayer is estimated from literature data [3,30,31] by assuming that α should be associated with the two dipole groups of the F_8H_{18} molecules, i.e., the terminal CF_3 and the CH_2-CF_2 junction groups. Israelachvili [31] gives the electronic polarizability of a C-F bond as $0.55 \times 4\pi\epsilon_0 \text{ \AA}^3$ and the electronic polarizability of a C-H bond as $0.65 \times 4\pi\epsilon_0 \text{ \AA}^3$. As an upper limit, α may be calculated as the following:

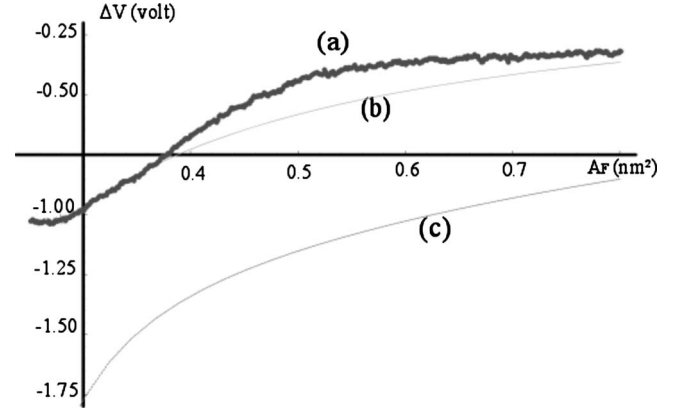


FIG. 6. Measured $\Delta V(\text{mV})-A_F(\text{nm}^2)$ isotherm diagram (curve a) and calculated ones (curves b and c). A good agreement is obtained when considering the apparent dipole moment μ_F/ϵ_F in Eq. (3) as constant and equal to the obtained experimental value $\mu_F/\epsilon_F = -0.78 \text{ D}$ (curve b), unlike the case where ϵ_F is considered as a function of the intermolecular distance a given in Eq. (5).

$$\begin{aligned} \alpha &\equiv \frac{\alpha_{CF_3} + \alpha_{CH_2-CF_2}}{2} \\ &\simeq \frac{3 \times \alpha_{CF} + 2 \times \alpha_{CF} + 2 \times \alpha_{CH}}{2} \\ &\simeq 2.2 \times 4\pi\epsilon_0 \text{ \AA}^3. \end{aligned} \quad (6)$$

We plot in Fig. 6 the experimental $\Delta V-A_F$ isotherm diagram obtained for $R=3.68$ (curve a) and the calculated ones (curves b and c). As we can notice, there is a good agreement between the experimental and the calculated $\Delta V-A_F$ isotherm diagrams in the case where ϵ_F is considered constant, unlike the case where ϵ_F is considered as a function of the intermolecular distance.

IV. CONCLUSION

We have shown in this paper by combining surface pressure, surface potential measurements, and atomic force microscopy that mixed films made of a nonhydrophilic semifluorinated F_8H_{18} molecules spread on the hydrophobic top of an alamethicin Langmuir monolayer constitute a very interesting experimental model which allows for a good agreement between measured and calculated surface potential isotherm diagrams. The particular chemical structure of F_8H_{18} molecules, the suitable structure of the underlying alamethicin monolayer and its collapse properties, allow for a continuous compression of the upper F_8H_{18} monolayer while the density of the lower alamethicin monolayer remains constant. We show also that the relative dielectric constant of the F_8H_{18} monolayer does not vary upon compression in this particular system. We attribute this result to the self-aggregation of F_8H_{18} molecules in nanosized circular domains whose size remains constant upon compression as observed by atomic force microscopy.

- [1] G. L. Gaines, Jr., *Insolubles Monolayers at Liquid-Gas Interface* (Interscience, New York, 1966).
- [2] J. T. Davies and E. K. Rideal, *Interfacial Phenomena* (Academic, New York, 1961).
- [3] D. M. Taylor and G. F. Bayes, *Phys. Rev. E* **49**, 1439 (1994).
- [4] D. M. Taylor, O. N. Oliveira, Jr., and H. Morgan, *Thin Solid Films* **173**, L141 (1989).
- [5] R. J. Demchak and T. J. Fort, Jr., *J. Colloid Interface Sci.* **46**, 191 (1974).
- [6] O. N. Oliveira, Jr., D. M. Taylor, T. J. Lewis, S. Salvagno, and C. J. M. Stirling, *J. Chem. Soc., Faraday Trans. 1* **85**, 1009 (1989).
- [7] J. F. Rabolt, T. P. Russell, and R. Twieg, *Macromolecules* **17**, 2786 (1984).
- [8] W. Mahler, D. Guillon, and A. Skoulios, *Mol. Cryst. Liq. Cryst. Lett.* **2**, 111 (1985).
- [9] C. Viney, T. P. Russell, L. E. Depero, and R. J. Twieg, *Mol. Cryst. Liq. Cryst. (Phila. Pa.)* **63**, 168 (1989).
- [10] J. Höpken and M. Möller, *Macromolecules* **25**, 2482 (1992).
- [11] G. L. Gaines, *Langmuir* **7**, 3054 (1991).
- [12] B. P. Binks, P. D. I. Fletcher, S. N. Kotsev, and R. L. Thompson, *Langmuir* **13**, 6669 (1997).
- [13] P. Marczuk, P. Lang, and M. Möller, *Colloids Surf., A* **163**, 103 (2000).
- [14] Y. Hayami and H. Sakamoto, *Colloid Polym. Sci.* **282**, 461 (2004).
- [15] M. P. Krafft, F. Giulieri, P. Fontaine, and M. Goldmann, *Langmuir* **17**, 6577 (2001).
- [16] A. I. El Abed, R. Ionov, M. Daoud, and O. Abillon, *Phys. Rev. E* **70**, 051607 (2004).
- [17] A. I. El Abed, R. Ionov, and M. Goldmann, *Phys. Rev. E* **76**, 041606 (2007).
- [18] R. Ionov, A. I. El Abed, A. Angelova, M. Goldmann, and P. Peretti, *Biophys. J.* **78**, 3026 (2000).
- [19] R. Ionov, A. I. El Abed, M. Goldmann, and P. Peretti, *J. Phys. Chem. B* **108**, 8485 (2004).
- [20] M. Broniatowski, I. Sandez Macho, and P. Dynarowicz-Latka, *Thin Solid Films* **493**, 249 (2005).
- [21] Fujiwara *et al.*, *Mol. Cryst. Liq. Cryst. (Phila. Pa.)* **441**, 307 (2005).
- [22] I. R. Peterson, *Rev. Sci. Instrum.* **70**, 3418 (1999).
- [23] Z. Huang, A. A. Acero, N. Lei, S. Rice, Z. Zhang, and M. Schlosmann, *J. Chem. Soc., Faraday Trans.* **92**, 545 (1996).
- [24] A. I. El Abed, E. Pouzet, M.-C. Fauré, M. Sanière, and O. Abillon, *Phys. Rev. E* **62**, R5895 (2000).
- [25] A. El Abed, M.-C. Fauré, E. Pouzet, and O. Abillon, *Phys. Rev. E* **65**, 051603 (2002).
- [26] M. Maaloum, P. Muller, and M.-P. Krafft, *Angew. Chem., Int. Ed.* **41**, 4331 (2002).
- [27] P. Lo Nostro, *Curr. Opin. Colloid Interface Sci.* **8**, 223 (2003).
- [28] M. Broniatowski and P. Dynarowicz-Latka, *Adv. Colloid Interface Science* **138**, 63 (2008).
- [29] J. R. Macdonald and C. A. Barlow, Jr., *J. Chem. Phys.* **39**, 412 (1963).
- [30] M. Iwamoto, Y. Mizutani, and A. Sugimura, *Phys. Rev. B* **54**, 8186 (1996).
- [31] J. M. Israelachvili, *Intermolecular and Surface Forces*, 2nd ed. (Academic Press, San Diego, 1987), p. 54.